Explicit expressions for elastic constants of osteoporotic lamellar tissue and damage assessment using Hashin failure criterion

R. Megías[*], R. Belda[*], A. Vercher-Martínez[*,†] and E. Giner[*,†]

[*] Institute of Mechanical and Biomechanical Engineering (I2MB)
Universitat Politècnica de València
Valencia, Spain
[†] Department of Mechanical Engineering and Materials (DIMM)
Universitat Politècnica de València
Valencia, Spain
e-mail: ramedia@upv.es; ribelgon@upv.es; anvermar@dimm.upv.es; eginerm@mcm.upv.es

Key words: lamellar bone tissue, microporosity, bone mineral density, elastic constants, bone tissue damage, finite element method

Abstract: *In this work, we have derived explicit expressions to estimate the orthotropic elastic constants of lamellar tissue as a function of the porosity at tissue level (microporosity) and the bone mineral density. Our results reveal that the terms of the main diagonal of the stiffness matrix fit an exponential equation, while the cross terms of the matrix fit a polynomial expression. Regarding to bone damage, failure onset assessed by Hashin criterion is mainly due to matrix elements failure. Finally, a linear relationship was found between bone mineral density (BMD) and cancellous bone stiffness at the macro scale.*

1 INTRODUCTION

Bone is a biological material with a hierarchical structure that develops in an optimal condition, supporting the loads to which it is subjected using the minimum material. Specifically, cancellous bone is a highly porous and heterogeneous material whose structure is mainly struts and plates framework. This type of bone is laminated at the microscale and the tissue arranged at these layers is called lamellar bone tissue.

At tissue level, collagen fibrils are known to be oriented in the direction of the strut on the most external surface [1]. However, as we move deeper into the strut towards the inside, the collagen is more randomly distributed. For this reason, the need to orient the material properties arises because the behaviour will not be the same in each direction. This non-isotropic nature of lamellar tissue must be considered in the quantification of bone mechanical properties.

On the other hand, porosity at lamellar tissue (microporosity) and bone mineral content are two relevant parameters related to bone mechanics. It is known that an increase of bone mineral density (BMD) implies a stiffness rise, but an excessive increase will make the lamellar tissue more brittle. Microporosity contributes in the bone loss mechanical response. Porosity exerts strong influences on mechanical properties in structural materials [2, 3]. Similar dependencies exist for bone, its strength and stiffness vary inversely with increasing porosity [4, 5]. Bone porosity has two possible sources, natural porosity and pathological such as osteoporosis. Natural porosity is mainly due to canaliculi, lacunae and vascular porosity. Pathological porosity causes a widening of vascularisation channels, increase of empty lacunae due to death of osteocytes and degradation in bone architecture.

As regards bone damage assessment, some researchers have defined isotropic failure criteria for assessing bone failure. In line with the previous comments, lamellar tissue has a non-isotropic behaviour, so we may need a more complex failure criterion. In composite materials, interactive failure criteria are usually used to model damage initiation in a composite layer. In 1980 Hashin

https://doi.org/10.4995/YIC2021.2021.12442

[6] proposed two failure mechanisms based on the matrix and fiber failure respectively and distinguished between tension and compression for unidirectional fiber composites. Failure of these type of material fits with the lamellar tissue failure, so we will study bone damage by Hashin's orthotropic failure criterion.

Finally, failure analysis requires the strength limits of the material. Ascenzi and Bonucci conducted several studies of different osteon types in order to define their strength limits [7, 8, 9]. They carried out tensile tests and they concluded that the osteons with longitudinal arrangement in the consecutive lamellae are the stiffest ones [7]. Under compression, osteons with a transverse arrangement of the collagen fibrils are the stiffest [8]. Under shear loads [9], osteons with some transverse collagen fibril arrangement were found to be stiffer in relation to the other types, such as longitudinal osteons.

In this work, we have estimated expressions for the orthotropic elastic constants of lamellar tissue as a function of the porosity at the tissue level and the bone mineral density. For this task, we have developed finite element models in which porosity is explicitly modelled as ellipsoids and spheres. Moreover, bone failure onset has been modeled by Hashin criterion, while damage evolution has been assessed through the material property degradation method (MPD).

2 MATERIALS AND METHODS

2.1 Specimen description, scanning and numerical modelling

A swine lumbar trabecular bone sample will be modelled for assessing bone damage. The trabecular bone sample was prepared in Instituto de Biomecnica de Valencia (IBV) from a lumbar vertebrae of a mature skeletal swine. The specimen was cut in parallelepiped-shaped sample with 10 mm length side. The sample was scanned by μ-CT in Estacin de Bioloxa Maria from A Graa (Universidad de Santiago de Compostela), whose scanner is Skyscan1172 (Bruker, Kontig, Belgium) achieving images with an isotropic resolution of 13.58 μm (voltage 100 kV, intensity 100 μA, Al/Cu filter). The μ-CT images were segmented using a manual global thresholding procedure (ScanIP, Simpleware, UK). From the set of μ-CT images of the scanned sample, a 2 mm cube-shaped region of interest was digitally extracted for the subsequent numerical model generation.

Numerical simulations of tension and compression load cases will be conducted. We consider three values of bone mineral density (BMD) in this study, 0.653 g/cm^3, 0.85 g/cm^3 and 1.16 g/cm^3, in order to evaluate BMD influence in the mechanical response. BMD and porosity will be implicitly considered using explicit expressions for the stiffness matrix at bone tissue level, derived in this work. For damage bone assessment, the strength limits, shown in Table 1, were inferred from [8, 10]. In the simulations, the main growth direction of bone is defined as the longitudinal direction of the sample where plates structure dominate, while the remaining two directions are defined as transverse directions where struts prevail.

Table 1: Strength limit values (MPa) for lamellar tissue. The subscript t, c and s denote tension, compression and shear, respectively.

S_{1t}	S_{1c}	$S_{2t} = S_{3t}$	$S_{2c} = S_{3c}$	$S_{12s} = S_{13s}$	S_{23s}
120	-115	50	-160	46	38

2.2 Modelling porosity in lamellar tissue

We have modelled the two types of porosity: natural (due to lacunae) and pathological. In order to mimic natural porosity we have modelled ellipsoids, which represent the empty lacunae after osteocytes death. On the other hand, we have used spheres for mimicking lamellar tissue

holes due to osteoporosis. Natural porosity represents up to a 10% of the total bone porosity [11]. Therefore, we assume ellipsoid voids up to a 5% porosity and spherical voids for the whole range of porosities.

We have studied six percentages of porosity (1%, 5%, 10%, 15%, 20% and 25%) according to Martnez-Reina [11] and twelve levels of bone mineral density. The minimum value we consider for the BMD at tissue level is 0.653 g/cm^3 from Koller [12], while the maximum value is 1.50 g/cm^3 from [13].

Porosity does not appear with any pattern neither with a specific arrangement in bone tissue. For this reason, we have generated ten models with a random distribution of non-overlapping spheres to represent pores at tissue level while we used ellipsoids to mimic lacunae, see Figure 1. An average stiffness matrix is assessed for the ten random models of each pair of porosity and BMD values.

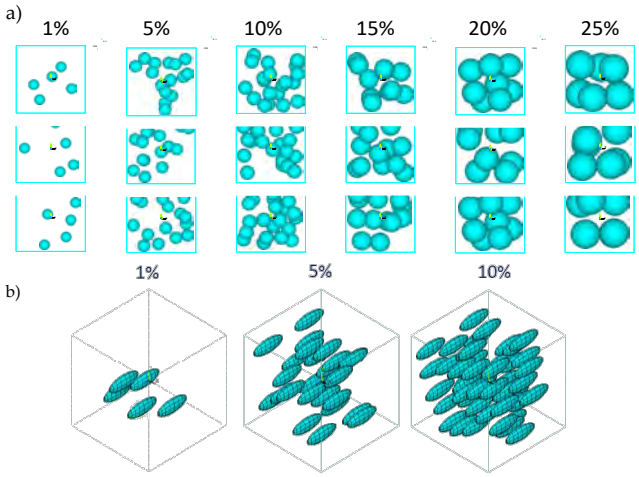

Figure 1: a) Random models with sphere-shaped pores and b) random models with ellipsoids

The reason why we have studied porosity with ellipsoids only until 5% is because they represent the lacunae which appear after osteocytes death. This type of porosity is due to natural bone porosity and it only represents at most the 5% of the total bone porosity. Regarding to sphere-shaped voids, we can model the whole range of porosity with them because with a little radius they represent natural bone porosity and with a larger radius they represent the holes that osteoporosis let at lamellar tissue.

The starting point of the current numerical model is considering the equations for estimating the elastic constants of a healthy bone as a function of the trabecular bone mineral density (BMD) in a multiscale approach [14].

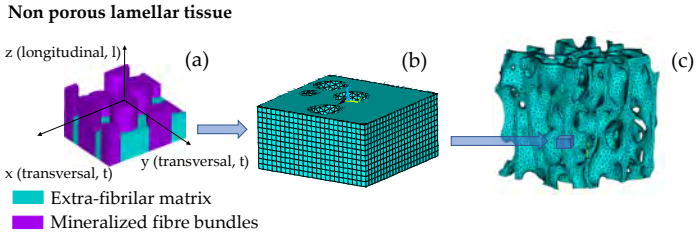

Figure 2: a) Transversely isotropic elastic properties of lamellar tissue as a function of BMD at tissue level [14]. b) Numerical model of the representative elementary volume of porous lamellar tissue. c) Trabecular bone numerical model at microscale.

Vercher et al. [14] assumed the lamellar tissue as a transversely isotropic material (Figure 2a). The elastic constants of the lamellar bone are given in [14].

The geometry of the numerical model is a region of interest of trabecular bone and is cube-shaped. We have modelled a representative periodically repeated volume called unit cell (Figure 2b). For this reason, we have applied periodic boundary conditions to guarantee that the analyzed hexahedron behaves as a continuous domain. Owing to the non-isotropic behaviour of lamellar tissue, the element coordinate system in the numerical model must be conveniently aligned with lamellar tissue properties. Regarding to the mesh, it is an important point of the numerical model due to the necessity of having a mirror mesh at each opposite faces of the model. Finally, a direct homogenization technique has been applied for estimating the average apparent stiffness of porous lamellar tissue.

2.3 Bone damage modeling

In this work, independent quasi-static load cases are numerically simulated. Bone failure onset has been modelled by Hashin's orthotropic failure criterion. On the other hand, bone damage evolution has been assessed through the material property degradation (MPD) method.

Hashin failure criterion is widely used to predict intralaminar failure in orthotropic materials. It assumes different failure mechanisms for tension and compression, both in the fiber and transverse directions. The formulation is the following [6]:

$$f_f = \left(\frac{\sigma_{11}}{X_t}\right)^2 + \frac{1}{S^2}\left(\tau_{12}^2 + \tau_{13}^2\right); \quad \sigma_{11} > 0 \tag{1}$$

$$f_f = \frac{\sigma_{11}}{X_c}; \quad \sigma_{11} < 0 \tag{2}$$

$$f_m = \frac{\left(\sigma_{22} + \sigma_{33}\right)^2}{Y_t^2} + \frac{\left(\tau_{23}^2 - \sigma_{22}\sigma_{33}\right)}{Q^2} + \frac{\left(\tau_{12}^2 + \tau_{13}^2\right)}{S^2}; \quad \sigma_{22} + \sigma_{33} > 0 \tag{3}$$

$$f_m = \frac{\left(\sigma_{22} + \sigma_{33}\right)}{Y_c}\left[\left(\frac{Y_c}{2Q}\right)^2 - 1\right] + \frac{\left(\sigma_{22} + \sigma_{33}\right)^2}{4Q^2} + \frac{\left(\tau_{23}^2 - \sigma_{22}\sigma_{33}\right)}{Q^2} + \frac{\left(\tau_{12}^2 + \tau_{13}^2\right)}{S^2}; \quad \sigma_{22} + \sigma_{33} < 0 \tag{4}$$

where X and Y are axial strength limits in longitudinal direction and transverse to the fiber, respectively ($X_t = S_{1t},\ X_c = S_{1c},\ Y_t = S_{2t},\ Y_c = S_{2c}$). Subscripts f and m denote fiber and matrix while subscripts t and c denote tension and compression. Furthermore, S and Q are shear strength limits in 12 and 23 planes respectively, being *1* the longitudinal direction of the fiber, normal direction to 23 plane ($S = Ss_{12},\ Q = Ss_{23}$).

We evaluate failure using the safety factor *f*, given by equation 5. Failure occurs for f values are greater than one.

$$f = max(f_f, f_m) \tag{5}$$

On the other hand, damage evolution is modelled through material property degradation. The load is progressively applied in quasi-static step increments until failure conditions are reached. Then the Young's modulus of the damaged elements is reduced.

In this work, the stiffness penalty for fiber and matrix failure is reduced differently. Fibers are stiffer and more resistant than matrix, so they transfer more load. If fibers fail, their stiffness is reduced in a 90%. On the other hand, if matrix fails, its stiffness is reduced to 50%.

3 RESULTS AND DISCUSSION

3.1 Expressions for the terms of the stiffness matrix as a function of porosity and bone mineral density

A non-linear multivariable regression by means of the least square fitting has been performed to adjust explicit expressions for the elastic constants of lamellar tissue as a function of the volumetric bone mineral density and porosity. For both porosity geometries, spheres and ellipsoids, the expressions estimated for the main diagonal of the stiffness matrix fit an exponential expression, equation 6.

$$y = ae^{b \cdot p} e^{c \cdot BMD} \tag{6}$$

Table 2: Values a, b and c for fitting the expression for the main diagonal for the stiffness matrix [C]. All the terms are expressed in GPa, BMD in g/cm^3 and porosity in %.

	Spheres			Ellipsoids		
	a	b	c	a	b	c
C_{11}	5.847	-0.02173	0.5817	5.757	-0.03656	0.5986
C_{22}	5.839	-0.02181	0.5830	5.784	-0.02004	0.6017
C_{33}	7.388	-0.02223	0.8213	7.119	-0.01527	0.8718
C_{44}	1.467	-0.02058	0.8123	1.336	-0.01318	0.8980
C_{55}	1.468	-0.02060	0.8119	1.334	-0.02199	0.8985
C_{66}	1.348	-0.02013	0.7298	1.254	-0.02277	0.7945

The exponential equation terms that fit equation 6 for each type of porosity are given in Table 2. The values which multiply the porosity are negative while those which multiply BMD are positive. Therefore, an increment of porosity in lamellar tissue causes a reduction of stiffness, while in bone mineral density leads to a stiffer material.

Figure 3 shows the terms of the main diagonal of the stiffness matrix for several bone mineral densities obtained with the estimated expressions for ellipsoids (cross markers) and sphere-shaped pores (circle markers). As can be seen, results for both expressions are really close between them, so we can use both indifferently. Moreover, the results for the term C_{33} are the highest in agreement with the most stiffest direction of the sample, the fibers direction. Besides, the terms C_{11} and C_{22} are almost identical according to the definition of the material which is transversely isotropic. Furthermore, it can be noticed that there is not a wide variation between the terms C_{44}, C_{55} and C_{66} of the main diagonal of the stiffness matrix.

The terms of the stiffness matrix [C] related to mutual influence and Chentsov coefficients are negligible in comparison with the rest of the terms and they only have a slightly variation with porosity and BMD. In order to complete the terms of the stiffness matrix we have to fit expressions for C_{12}, C_{13} and C_{23} terms. A polynomial function is the best fit for the numerical results obtained, but with slightly differences between spheres and ellipsoids holes. Equation 7 shows the fitting expression used for spheres-shaped pores, while equation 8 the corresponding for ellipsoids pores. Table 3 summarizes the values which correspond with each term of the fitting equation.

$$y = a + b \cdot p + c \cdot p^2 + d \cdot p^3 + e \cdot BMD + f \cdot BMD^2 + g \cdot BMD^3 \tag{7}$$

$$y = a + b \cdot p + c \cdot p^2 + d \cdot p \cdot BMD + e \cdot BMD + f \cdot BMD^2 \tag{8}$$

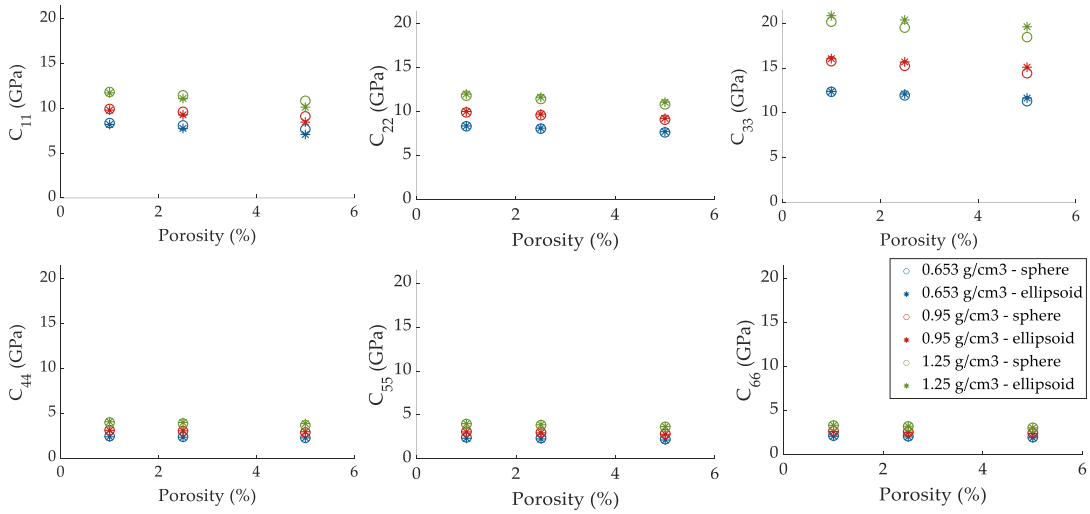

Figure 3: Comparison between the expressions estimated for the terms of the main diagonal of the stiffness matrix for mimicking porosity by ellipsoids and sphere-shaped holes.

Table 3: Values for the parameters a, b, c, d, e, f and g for fitting the polynomial expressions. All the terms are expressed in GPa, BMD in g/cm^3 and porosity in %. Subscript s denotes the spheres terms and subscript e denotes ellipsoids terms.

	a	b	c	d	e	f	g
$C_{12,s}$	2.1878	-0.12627	8.402210^{-4}	0	4.0292	-1.1405	0
$C_{13,s}$	-3.6721	-0.10889	-6.156610^{-4}	3.635010^{-5}	19.131	-10.812	0.58818
$C_{23,s}$	-6.6623	-0.11082	-3.934510^{-4}	3.022710^{-5}	30.459	-25.596	7.0279
$C_{12,e}$	0.7633	-0.1727	0.004519	-0.03203	6.949	-2.633	-
$C_{13,e}$	-1.261	-0.2131	0.004492	0.005465	12.67	-6.059	-
$C_{23,e}$	-1.486	-0.1581	0.002377	0.01366	13.15	-6.305	-

Figure 4 plots the results for the cross terms of the stiffness matrix. Both C_{13} and C_{23} terms show the same trend for the results. For these terms, the function has a maximum and then falls again, hence, the results for 0.95 g/cm^3 are greater than the ones for 1.25 g/cm^3. On the other hand, the equation followed for C_{13} is a polynomial that for all the studied values always grows. Therefore, as BMD increases the results increase as well.

3.2 Failure modeling results for tension and compression load cases

In this section, we have studied the failure behaviour of a vertebral trabecular swine bone numerical model. Figure 5 shows the results considering a 0.85 g/cm^3 bone mineral density and 5% of porosity. Tension load case is represented in blue whereas orange corresponds to the compression load case. Dashed lines represent the hypothetical linear behaviour of the sample in order to identify failure onset. The sample has a similar behaviour under tension and compression loads. However, the failure onset begins a bit earlier in tension than in compression. Moreover, the maximum stress is higher for compression than for tension.

The elements that fail under compression load at yielding and complete failure are represented in red in Figure 5. It can be noted that few elements failed at yielding, mainly due to matrix failure. After several load steps, the material collapses and several elements failed. Their stiffness has been reduced as compression has progressed. At this point, the component is not able to bear greater strains and collapses.

Three different values of BMD have been chosen for evaluating its influence on the failure

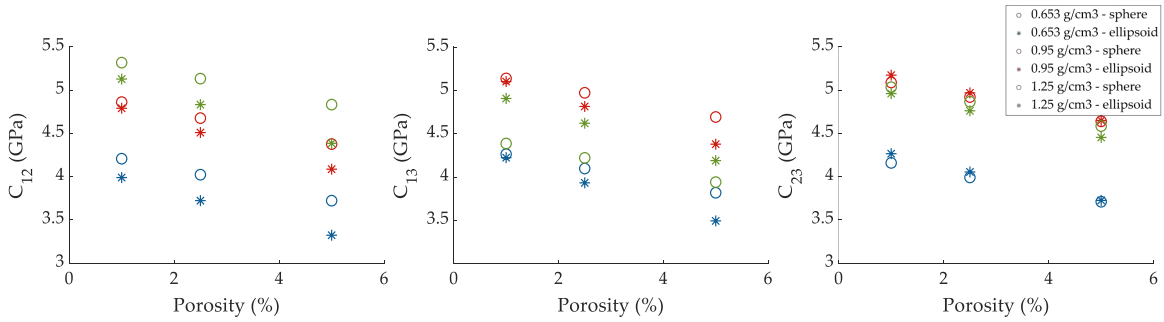

Figure 4: Comparison between the expressions estimated for the cross terms of the stiffness matrix for mimicking porosity by ellipsoids and sphere-shaped holes.

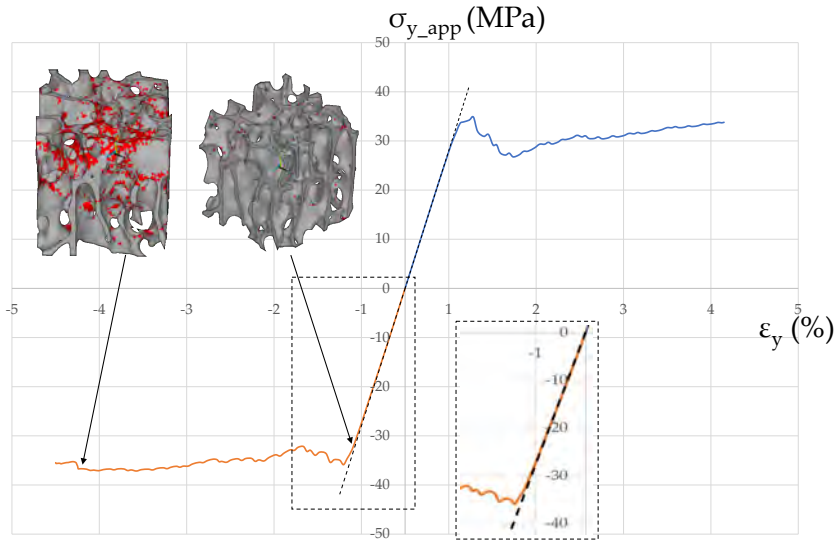

Figure 5: Tension and compression curves for the longitudinal direction (bone growth main direction) for a vertebral trabecular swine bone numerical model with 0.85 g/cm^3 bone mineral density and 5% of porosity.

of the vertebral trabecular swine bone. Porosity has been set for all cases in 5% because this percentage corresponds to a healthy bone, and there was no evidence about the presence of any disease or pathology in the animal.

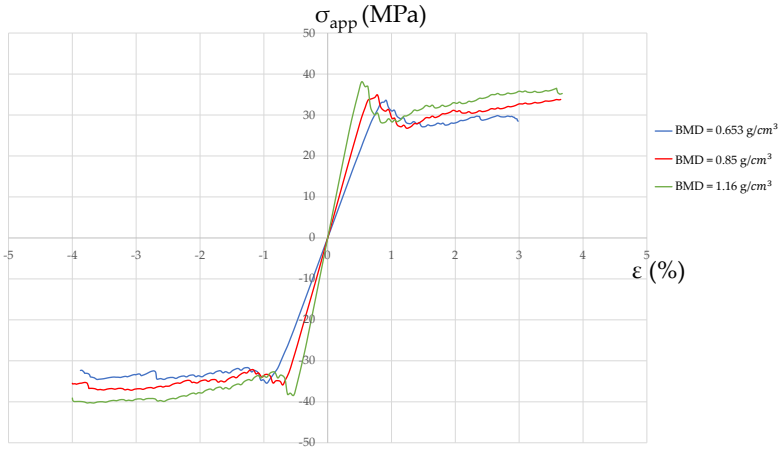

Figure 6: Tension and compression behaviour curves for three values of bone mineral density.

Figure 6 shows the tension-compression response of the cancellous bone specimen for three BMD values. As can be seen in the reported results, as BMD increases, the apparent stress that sample can withstand is greater. The reason is due to the fact that bone mineral density contributes to a higher stiffness in bone. It can be observed that as bone mineral density increases, yield strain is lower, but the apparent stress that each sample can withstand at the yield point is greater as stiffness increases.

4 CONCLUSIONS

In this work, we provide explicit expressions for the terms of the stiffness matrix as a function of porosity and bone mineral density. We have mimicked natural porosity at tissue level using ellipsoids due to the lacunae voids after osteocytes death and spheres for both sources of porosity, natural and pathological. The terms of the main diagonal of the stiffness matrix follow an exponential equation, whereas the cross terms fit a polynomial law. The results obtained indicate that an increment of porosity in lamellar tissue causes a reduction of stiffness, while in bone mineral density leads to a stiffer material.

We have detected that the importance of orientating the lamellar tissue in the numerical models is essential for obtaining results closely to an experimental test. The structure of the vertebral trabecular swine bone sample has dominant struts structure in the transverse directions, while plates prevail in the main growth direction of bone. For this reason, we have oriented the fibers vertically in plate directions and flat for transverse directions where struts exist.

Finally, we have proved that an orthotropic failure criterion can be used in order to analyse bone failure onset considering bone tissue as a composite material. Moreover, elastic property degradation method is an efficient procedure to analyse the failure propagation in a 3D numerical model due to its computational cost. Stress - strain curves for the trabecular bone numerical model show a similar behaviour both in tension and compression. Furthermore, the influence of BMD on the stiffness of the trabecular bone has been studied and we have seen that as BMD increase the apparent stiffness of the sample is greater.

ACKNOWLEDGEMENTS

The authors acknowledge the Generalitat Valenciana for the financial support received through Plan FDGENT 2018. The authors also ackowledge the Ministerio de Ciencia e Innovacin and the ERDF-FEDER programme through the project DPI2017-89197-C2-2-R.

REFERENCES

[1] Georgeadis, M. et al. Ultrastructure organization of human trabeculae assessed by 3D sSAXS and relation to bone microarchitecture. *Plos One*, 11 (8), e0159838, (2016).

[2] Hashin, Z. The elastic moduli of heterogeneus materials. *J. Appl. Mech.*, 29, 143-150, (1962).

[3] Brown, S., Biddulph, R.B. and Wilcox, P.D. A strenght - porosity relation involving different pore geometry and orientation. *Am. Ceram. Soc. J.*, 47, 320, (1964).

[4] Carter, D.R. and Hayes, W.C. The compressive behaviour of bone as a two - phase porus structure. *J. Bone Jt. Surg.*, 59A, 954-962, (1977).

[5] Martin, R.B. Porosity and specific surface of bone. *CRC Crit. Biomed. Engng.*, 10, 179-222, (1984).

[6] Hashin, Z. Failure criteria for unidirectional fiber composites. *J. Appl. Mech.*,Vol. 47, pp. 329-334, (1980).

[7] Ascenzi, A. and Bonucci, E. The tensile properties of single osteons. *The Anatomical Record*, 161(3):377-391, (1967).

[8] Ascenzi, A. and Bonucci, E. The compressive properties of single osteons. *The Anatomical Record*, 161(3):377-391, (1968).

[9] Ascenzi, A. and Bonucci, E. The shearing properties of single osteons. *The Anatomical Record*, 161(3):377-391, (1972).

[10] Giner, E., Arango, C., Vercher, A. and Fuenmayor, F.J. Numerical modelling of the mechanical behaviour of an osteon with microcracks. *Anat. Rec.*, 161:377-392, (2014).

[11] Martínez-Reina, J., Domínguez, J. and García-Aznar, J.M. Effect of porosity and mineral content on the elastic constants of cortical bone: a multiscale approach. *Biomech. Model. Mechanobiol.*, 10:309-322, (2011).

[12] Koller, B. and Laib, A. Calibration of micro-CT data for quantifying bone mineral and biomaterial density and microarchitecture. *Advance Bioimagin Technologies in assessment of the quality of bone and scaffold materials: Techniques and Applications*, DOI: 10.1007/978-3-540-45456-4-5, (2007).

[13] Yu, W. et al. Spinal bone mineral assessment in postmenopausal women: a comparison between dual X-ray absorptiometry and quantitative computed tomography. *Osteoporosis Int.*, 5:433-439, (1995).

[14] Vercher-Martínez A., Giner, E., Belda, R., Aigoun, A. and Fuenmayor, F.J. Explicit expressions for the estimation of the elastic constants of lamellar bone as a function of the volumetric mineral contents using a multi-scale approach. *Biomech. Model. Mechanobiol.*, 17:449-464, (2017).